European Journal of Pharmaceutics and Biopharmaceutics 72 (2009) 332–338

Contents lists available at ScienceDirect

European Journal of Pharmaceutics and Biopharmaceutics

journal homepage: www.elsevier.com/locate/ejpb

Research paper

A comparison of two- and three-dimensional models for the simulation of the permeability of human stratum corneum

Arne Naegel, Michael Heisig, Gabriel Wittum *

Goethe-Center for Scientific Computing, Goethe-University, Frankfurt am Main, Germany

ARTICLE INFO

Article history:
Received 30 April 2008
Accepted in revised form 11 November 2008
Available online 28 November 2008

Keywords:
Stratum corneum
Cell shape
Three-dimensional models
Permeability
Numerical simulation
Cuboid
Tetrakaidekahedra
Homogenization

ABSTRACT

The stratum corneum is the outermost layer of cells in mammalian epidermis. It is widely believed to play the key role for the barrier function of the skin. This study characterises how the cell geometry influences the permeability of the membrane. It is based on a diffusion model, which is evaluated using numerical simulation. Three different geometry concepts, i.e., ribbon, cuboid and tetrakaidekahedral type, in two and three space dimensions are compared. The results confirm that tetrakaidekahedral cells with an almost optimal surface-to-volume ratio provide a barrier, in which a minimal amount of mass is used very effectively. Additionally, the study supplies tools to quantify this and links the results to the theory of homogenization.

1. Introduction

The stratum corneum (SC) is a biphasic membrane, typically about 15–20 μm thick, consisting of flattened and keratinized corneocyte cells and the surrounding inter-cellular lipid matrix. The barrier properties of the SC can be quantified by the permeability and the time lag.

Since the mid seventies of the last century, it has been a well known fact that the arrangement of cells in the upper epidermis and the stratum corneum can be described by tetrakaidekahedra [1–4]. The advent of high resolution imaging techniques confirms this shape and further allows to evaluate height and diameter, surface and volume of single cells [5–9].

On the other hand, in the meantime numerous works on mathematical modelling of the SC have been published. A survey is given, e.g., in [10]. However, except for the results in [11], the authors are not aware of a study that takes into account the tetrakaidekahedral shape in a three-dimensional model. The purpose of this work is to fill this gap: for the first time, permeabilities are computed on a realistic geometry, and the results are compared to the standard approaches in use.

Three-dimensional models are crucial to understand the diffusional pathway through the SC and the quantitative importance of the SC morphology for the barrier function.

2. Model geometries

This section introduces three different geometry models for the stratum corneum. All have in common a prototype for a corneocyte cell that is embedded in a lipid matrix. The SC membrane is then obtained by agglomeration, and allows to distinguish the corneocyte phase Ω_{cor} from the lipid phase Ω_{lip}. The parameterisation of the cells is then discussed for each geometry model individually, before a comparison of the models is supplied. Finally, a literature survey on realistic dimensions is supplied.

2.1. Ribbon

Standard approaches model a two-dimensional cross section of the SC, as depicted in Fig. 1. As the cells stretch infinitely into the neglected direction, we will refer to these geometries as of ribbon type, a term used, e.g., by Goodyer and Bunge [12]. Relevant parameters are the cell height h, the edge length w, and the lipid layer thickness d. Between two neighbouring layers, the horizontal overlap ω plays an important role. It is defined as the ratio between the shortest cell edge s_{cell} and its total width $w_{cell} = (w + d)$.

* Corresponding author. Goethe-Center for Scientific Computing, Goethe-university, Kettenhofweg 139, D-60325 Frankfurt am Main, Germany. Tel.: +49 69 798 25259.
E-mail address: wittum@gcsc.uni-frankfurt.de (G. Wittum).

0939-6411/$ - see front matter © 2009 Published by Elsevier B.V.
doi:10.1016/j.ejpb.2008.11.009

Nomenclature

D_{lip}	diffusion coefficient in the lipid phase
D_{cor}	diffusion coefficient in the corneocyte phase
$K_{cor/lip}$	partition coefficient between lipid and corneocyte phase
ξ	rescaled corneocyte diffusion coefficient, i.e., $\xi = K_{cor/lip} D_{cor}/D_{lip}$
θ_{lip}	relative volume fraction of the lipid phase
θ_{cor}	relative volume fraction of the corneocyte phase
$\alpha_{SC,\infty}$	maximum permeability multiplier, i.e., factor by which the permeability is larger than in the homogeneous case (larger or equal to unity)
$\alpha_{SC,0}$	minimum permeability multiplier, i.e., factor by which the permeability is smaller than in the homogeneous case (smaller or equal to unity)

2.2. Cuboid

A straightforward generalization of the above concept to three spatial dimensions is the cuboid model, as proposed, e.g., in [12–15]. A schematic diagram is found in Fig. 2. In what follows, we restrict ourselves to the case where cells in neighbouring layers undergo an identical shift in both planar directions. Regarding the morphology of the cells, this seems to be reasonable, as it assumes that there is no distinct direction.

2.3. Tetrakaidekahedra

The concept to use tetrakaidekahedra (TKD) as building blocks for cell geometries [1–4] dates back to a work by Lord Kelvin in the nineteenth century [16]. A detailed description of the tetrakaidekahedral model applied in this work is presented in [11,17,18].

The characterisation of a corneocyte cell requires three parameters, which are indicated in Fig. 3. In addition to the height h controlling the transversal extension, there are two quantities, a and w, controlling the lateral extension. While the edge length a controls the shape of the top and the bottom hexagon, the width w defines the distance of two corresponding edges between hexagons on the sides.

After adding a surrounding lipid matrix of thickness $d/2$, as illustrated in Fig. 4, one obtains a base cell T. A cluster P of three of these cells can be extended periodically in x- and y-direction. Thus, an arrangement in N layers yields a membrane of finite thickness, which stretches infinitely into the planar directions.

To specify the horizontal alignment for this model consistently with the previous definition, one may employ the (projected) distance b and the length s as shown in Fig. 3. By denoting the corresponding quantities for an embedded cell by b_{cell} and s_{cell}, the overlap is given by $\omega = s_{cell}/b_{cell}$.

2.4. Literature review

The experimental work by [5] investigated the swelling of cells in distilled water using tapping mode scanning force microscopy. The cell samples were taken from the inside of the forearm (close to wrist, topmost layers only). For dried cells, the authors report a cell diameter of 30–40 μm and a mean height of 0.2–0.3 μm. The area and volume are roughly 1000 μm^2 and 300 μm^3. Swelling is reported to increase height and volume by ≈50%. In a follow-up study [6], they report cell thicknesses between 0.5 and 1.5 μm.

Using FT infrared spectroscopy/cryo scanning electron microscopy, Bouwstra et al. [7] performed a similar study with human abdominal skin. The authors report a cell diameter of 20–30 μm and a cell height between 0.3 μm (dry) and 3.0 μm (hydration over pure water).

A study by [8] was performed with samples from the upper arm and the cheek, and reports surface areas in the range of 900–1000 μm^2. Depending on the body site, the reported heights are as low as 0.15 μm, and the cell volumes are in the range of 200 μm^3. However, in this case the corneocytes were pretreated with xylene and air dried afterwards.

Finally, the study in [9] focuses on the internal structure of the corneocytes. Nevertheless, the reported cell height and diameter are determined and reported to be in the range of 0.5–2 μm and 30–45 μm, respectively. In all works, no or only little swelling into horizontal directions is observed.

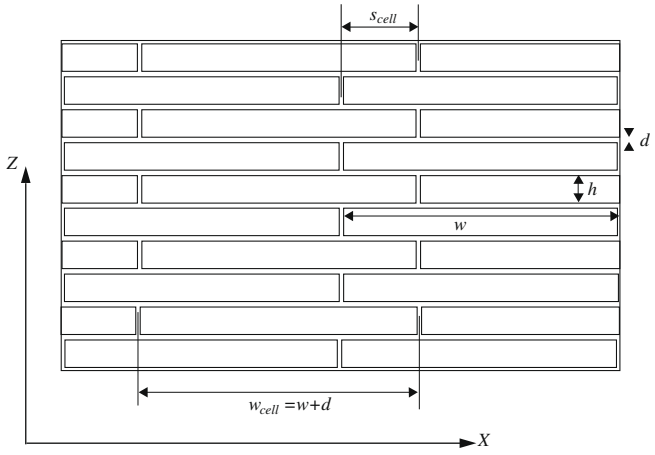

Fig. 1. Illustration of corneocyte cells of ribbon type embedded in the lipid matrix. Geometric parameters: edge length w, height h, lipid channel thickness d, and overlap $\omega = s_{cell}/w_{cell}$. The stack consists of $N = 10$ cell layers and allows periodic extension in lateral direction.

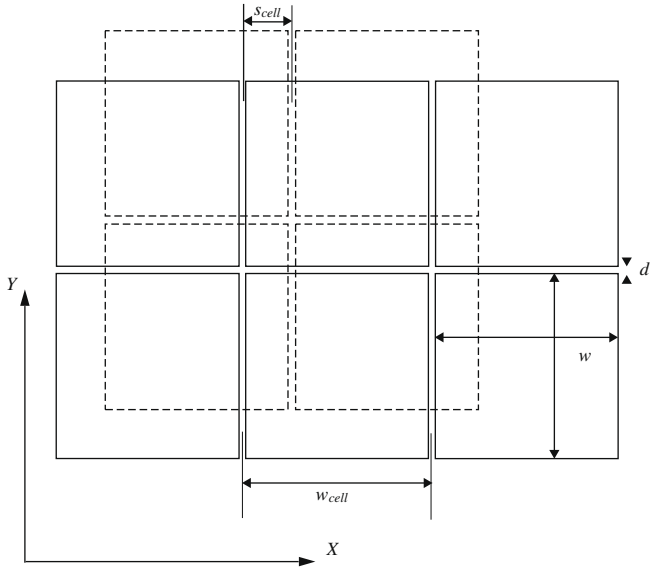

Fig. 2. Schematic top view onto two adjacent cell layers for cuboid-type membranes (redrawn from [13]).

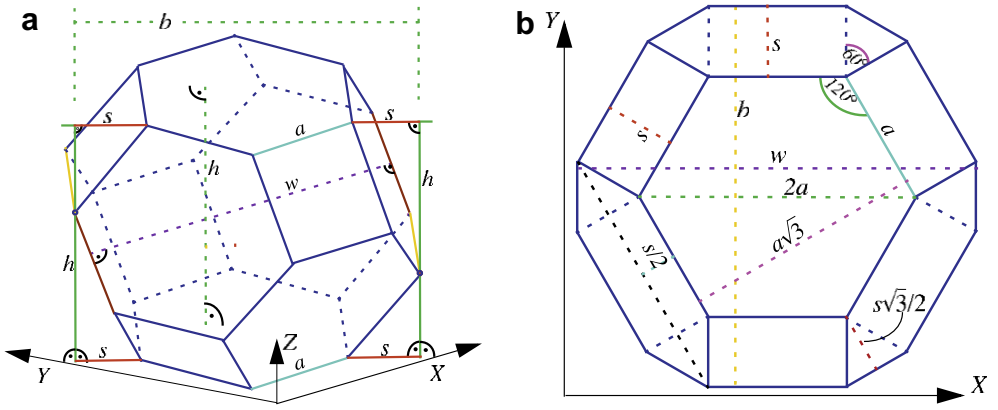

Fig. 3. Illustration of a corneocyte cell of TKD type in side view (a) and top view (b). Geometric parameters: height h, edge length a and width w. Redrawn from [18].

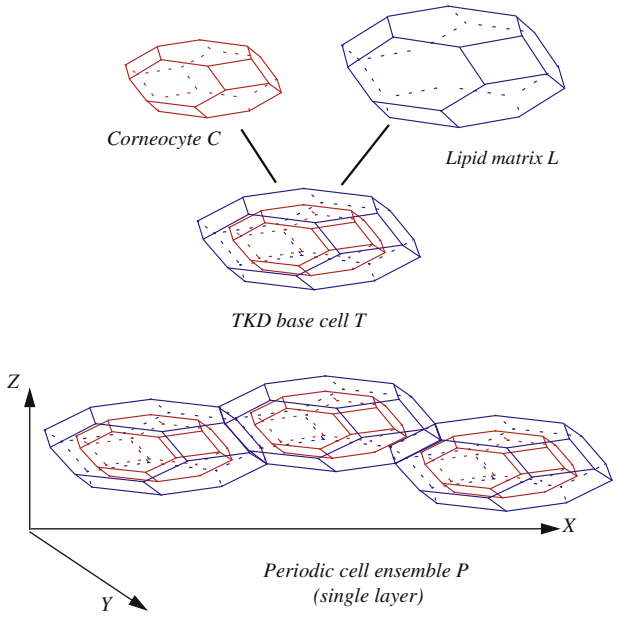

Fig. 4. Corneocytes C (as parameterised in Fig. 3) are embedded in a lipid matrix L, such that the distance of corresponding surfaces is $d/2$. The resulting base cell T is triplicated and agglomerated to a periodic cell P. A stack of $N = 10$ layers of cell P yield the computational domain.

An estimate for the dimensions of the lipid matrix is indirectly provided by the lipid content in the SC. Anderson and Cassidy [19] report a weight fraction of lipids of 20–30% for dry SC, while [20] determines a value around 15% under presumably natural environmental conditions. However, variabilities are large and, e.g., a dependence on the body site must be assumed.

In the field of modelling literature, a variety of parameters are used to characterise the cell shape of the corneocytes. Parameters are similar for the published computational models of brick-and-mortar type (i.e., ribbon and cuboid). An overview is provided in Table 1.

To conclude, it is consistent with the literature to assume a cell width of $w = 30\ \mu m$ and a height of $h = 1.0\ \mu m$. For the lipid channel, a thickness $d = 0.1\ \mu m$ is chosen. In what follows, the SC membrane consists of $N = 10$ layers of cells. This is at the lower end of what is reported in the literature, but still allows computations for the TKD model. However, as will be shown in the course of this work (cf. Fig. 8), the number of cell layers plays a subordinate role for $N \geqslant 8$.

2.5. Model comparison

It should be stressed that the overlaps ω are comparable for all three models, as all definitions only refer to the horizontal axes and yield values in the interval $(0, 0.5)$. However, especially for the TKD model, it is a weak approximation to the tortuosity, as it neglects the three-dimensional structure.

With respect to physiology, it is more important to consider the volume of the corneocytes. Regarding the influence of cell differentiation and thus the influence of the shape, it must be investigated whether cells with equal volumes yield comparable barrier properties. Table 2 contains a comparison of the three geometry models. The parameters of interest are the lipid volume V_{lip}, the corneocyte volume V_{cor}, and the corneocyte surface area A_{cor}. All quantities are given per base cell. The relative volume fractions $\theta_{lip} = V_{lip}/V_{cell}$, $\theta_{cor} = V_{cor}/V_{cell}$ are then defined using the cell volume $V_{cell} = V_{lip} + V_{cor}$.

Taking the TKD model geometries, e.g., with $w = 30\ \mu m$, $a = 8\ \mu m$, as a reference, we observe that a cuboid model with identical surface area must have an edge length $w \approx 25\ \mu m$. To obtain a geometry with identical volume, it requires to go down even to a value as low as $w \approx 20\ \mu m$. For the sake of completeness, the cuboid geometry proposed in [13] is also included.

Table 1
Overview of parameters in recently published brick-and-mortar models.

Reference	a (μm)	h (μm)	d (μm)	ω	Remark
Heisig et al. [21]	30	1.0	0.1	Variable	
Johnson et al. [22]	40	0.8	0.075	1/9	
Barbero and Frasch [23]	44	3.5	0.1	12/49	Swollen
Wang et al. [10]	30	0.8	0.081	Variable	Partially swollen
	31.2	2.8	0.081	Variable	Swollen
Rim et al. [13]	40	0.8	0.075	1/2	
Herein	30	1.0	0.1	Variable	

Table 2
Comparison of the model geometries. Given are the lipid and corneocyte volume V_{lip}, V_{cor}, the relative volume fractions θ_{lip}, θ_{cor} and the corneocyte surface area A_{cor} for a single corneocyte cell, embedded in the lipid matrix.

Geometry	w [μm]	a [μm]	V_{lip} [μm^3]	(θ_{lip}) (%)	V_{cor} [μm^3]	(θ_{cor}) (%)	A_{cor} [μm^2]
Ribbon (2D)	30		n.a.	(9.39)	n.a.	(90.61)	n.a.
Cuboid (3D)	30		96.61	(9.69)	900.00	(90.31)	1920.00
	25		68.01	(9.81)	625.00	(90.19)	1350.00
	20		44.41	(9.99)	400.00	(90.01)	880.00
	40*		125.25	(8.91)	1280.00	(91.07)	3328.00
TKD (3D)	30	8	76.23	(15.46)	416.85	(84.54)	1450.82
	30	10	72.10	(13.50)	461.88	(86.50)	1389.69
	30	13	64.86	(10.83)	533.76	(89.17)	1276.49

* Geometry from [13] with $h = 0.8$ μm and $d = 0.075$ μm. All other cases use $h = 1$ μm and $d = 0.1$ μm.

3. Model equations

An investigation of the barrier properties of the membranes just introduced in the previous section is the primary concern of this section. After introducing the model equations, the permeability as the primary characteristic quantity is investigated.

3.1. Diffusion model

It is assumed that the transport is diffusion driven, i.e., the following equation holds in each compartment $i \in \{lip, cor\}$:

$$\partial_t c_i(t,x) = div[D_i \nabla c_i(t,x)] \tag{1}$$

The diffusion-coefficients are piecewise constant, but are allowed to differ, $D_{cor} = \alpha_{cor} D_{lip}$. On the interface between both corneocyte and lipid phase, the concentration may undergo a discontinuity due to Nernst's law

$$c_{cor} = K_{cor/lip} c_{lip}, \tag{2}$$

with a constant partition coefficient $K_{cor/lip} = K$. Fluxes across the interface are preserved, i.e., $(D_{lip}\nabla c_{lip} + D_{cor}\nabla c_{cor}) \cdot n = 0$.

3.2. Characteristic quantity

The permeability is defined as the constant of proportionality between the steady state flux j_{SC} and the concentration difference $c_{lip,\delta}$ applied at the top and the bottom part of the membrane

$$j_{SC} = P_{SC} c_{lip,\delta}.$$

Note that the concentration $c_{lip,\delta}$ is defined in the lipid layers and does not account for partitioning from a donor medium. As

$$j^{(hom)} = D_{lip}/l c_{lip,\delta} \equiv P^{(hom)} c_{lip,\delta}$$

holds for a homogeneous membrane ($D_{cor} = D_{lip}, K_{cor/lip} = 1$) with thickness l, flux $j^{(hom)}$ and permeability $P^{(hom)}$, the ratio

$$\alpha_{SC} = j_{SC}/j^{(hom)} = P_{SC}/P^{(hom)}$$

is constant, and depends on the dimensionless constant $\xi = \alpha_{cor} K_{cor/lip}$ only. We will refer to α_{SC} as *flux* or *permeability multiplier* from now on.

3.3. Numerical methods

All computations were carried out in the software toolbox UG [24]. A linear finite volume scheme was used for the discretization, the accuracy of the computations was ensured by a consecutive refinement of elements. The error can be guaranteed to be well below 1% for the cuboid models, and below 10% for the TKD model. Due to the complex geometry of the latter one, more than 4.2×10^8 elements (corresponding to roughly 2.9×10^8 degrees of freedom) had to be employed in the worst case.

3.4. Homogenization

Using the theory of homogenization [13,25], one can formally reduce the system given by Eqs. (1) and (2) to an equation in the coarse-scale unknown $\hat{c}_0$

$$\rho(K)\partial_t \hat{c}_0(t,x) = div[\widehat{D}\nabla \hat{c}_0(t,x)]. \tag{3}$$

This unknown is an upscaled (or apparent) SC concentration and defined independently of lipid and corneocyte phase. The equation includes the effective mass coefficient

$$\rho(K) = \theta_{cor} K + \theta_{lip} \tag{4}$$

and the effective diffusion tensor $\widehat{D}$. The latter one is not a scalar, but a matrix. For instance,

$$\widehat{D} = \begin{pmatrix} D_{lat,x} & 0 & 0 \\ 0 & D_{lat,y} & 0 \\ 0 & 0 & D_{trans} \end{pmatrix}$$

for the cuboid model. Note that for the ribbon and cuboid geometry, the coefficient in transversal direction can be expressed as $D^{SC}_{trans} = \alpha_{SC} D_{lip}$. However, this does not necessarily hold for the TKD geometry.

A major drawback of the homogenization approach is that the error is of order $O(h_{cell} + w_{cell})$ when comparing the results to the solution of the original equations. Thus, the homogenized solution is valid only, if the cell height h_{cell} and the cell width w_{cell} are small with respect to the membrane thickness $l = N h_{cell}$, i.e., for membranes with a large number of layers N.

4. Results

In this section, we give results for the three different models and evaluate the efficiency of the membrane.

4.1. Permeability

As previously shown, the approximation

$$\alpha_{SC}(\xi) = \alpha_{SC,0} + \frac{(\alpha_{SC,\infty} - \alpha_{SC,0})(1 - \alpha_{SC,0})\xi}{(\alpha_{SC,\infty} - 1) + (1 - \alpha_{SC,0})\xi} \tag{5}$$

with $\xi = \alpha_{cor} K_{cor/lip}$ is very efficient to represent the permeability multiplier for the ribbon geometry [26,27]. Before showing that this also holds true for the cuboid and the TKD geometry, we briefly repeat an analysis of Eq. (5).

Besides the dimensionless model parameter ξ, the formula contains the geometry-dependent constants $\alpha_{SC,\infty}$ and $\alpha_{SC,0}$ only. The latter ones characterise the membrane in two important limit cases: For $\xi \to \infty$, the corneocytes provide an infinitely fast diffusion pathway resulting in a maximum multiplier $\alpha_{SC,\infty}$. For $\xi \to 0$, the diffusion occurs through the lipid channels only, leading to

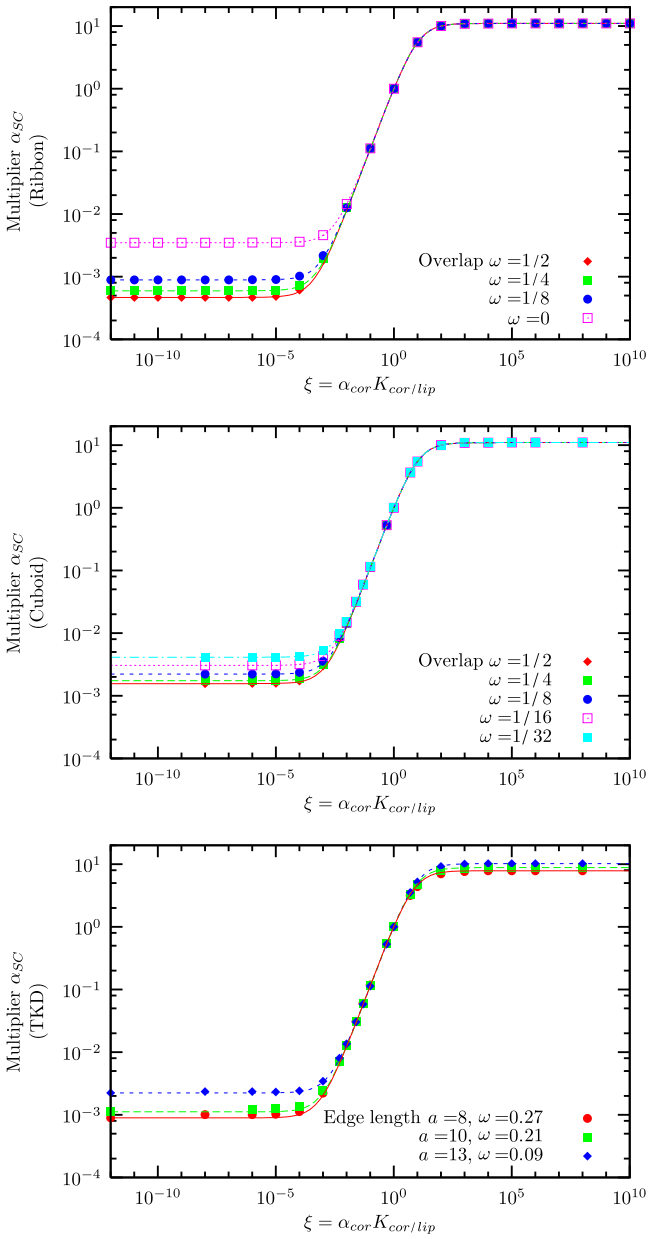

Fig. 5. Effective flux/permeability multiplier for ribbon (top, cf. [27]), cuboid (center) and TKD model (bottom) as a function of ξ. Markers indicate results of simulations, while straight lines are the corresponding approximation by Eq. (5).

the minimal permeability multiplier $\alpha_{SC,0}$. We emphasize that in chemical engineering a variety of closed form expressions have been developed to approximate $\alpha_{SC,0}$ for two-dimensional membranes, e.g., [28].

The illustrations in Fig. 5 contain simulated flux/permeability multipliers for a variety of values for ξ. Results of the simulations are given by markers, while the approximations by Eq. (5) are shown as lines. The graphs show that this yields excellent agreements for all the three models.

4.2. Membrane efficiency

To assess the efficiency of the model membranes, one can evaluate the dependence of the minimal flux multiplier $\alpha_{SC,0}$ on the overlap ω. For the three models, this is presented in Fig. 6. It is worthwhile mentioning that all the three models provide a very effective barrier for overlaps between 20% and 30% already.

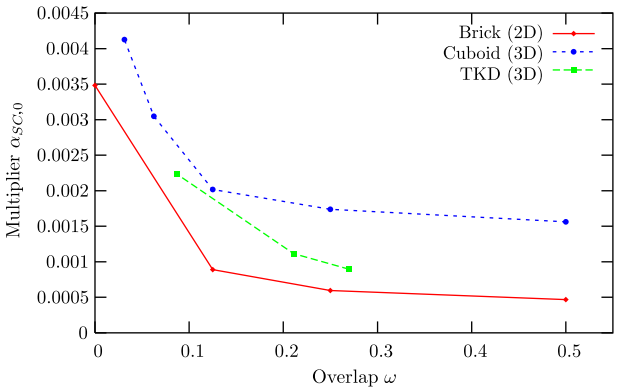

Fig. 6. Minimal flux/permeability multiplier $\alpha_{SC,0}$ depending on the overlap ω for ribbon, cuboid and TKD model geometry.

The key question from a biological point of view is how a low membrane permeability is obtained with a minimal amount of biological tissue. Hence, how the volume of the cells affects the minimum permeability value $P_{SC,0}$ is investigated in a next step. Since the cell-wise relative volume fractions are approximately constant, cf. Table 2, we use V_{cor} as a reference value. The TKD model with different edge lengths $a = 8$, 10, 13 μm and overlaps $\omega = 0.27$, 0.21, 0.09 is compared with its cuboid counterparts with different edge lengths $w = 20, 25, 30$ μm and full horizontal overlap $\omega = 0.5$. To complement the study, the geometry used by [13] ($w = 40$ μm, $h = 0.8$ μm, $d = 0.075$ μm) is also included. As usual, all membranes consist of $N = 10$ layers of cells. The results are shown in Fig. 7.

The most important observation is that the TKD-based geometries provide a better 'barrier per volume' trade-off than the cuboid-based ones. Note that in Fig. 7 the TKD model with edge length $a = 8$ μm has the smallest volume ($V_{cor} = 416.85$ μm^3) and shows the lowest permeability. This is due to the large overlap. The geometry is almost by a factor of two less permeable than the cuboid geometry with $w = 30$ μm ($V_{cor} = 900$ μm^3), and approximately three times less permeable than cuboid membranes with comparable corneocyte volume ($w = 20$ μm, $V_{cor} = 400$ μm^3; $w = 25$ μm, $V_{cor} = 625$ μm^3). Only the geometry with the parameterisation proposed in [13] ($w = 40$ μm, $V_{cor} = 1280$ μm^3, cf. Table 2) is comparable, but features a corneocyte volume which is approximately three times larger.

A variation of the number of cell layers N enables to study how the number of cell layers affects the permeability. As visualized in Fig. 8, this parameter plays a minor role, but cannot be neglected.

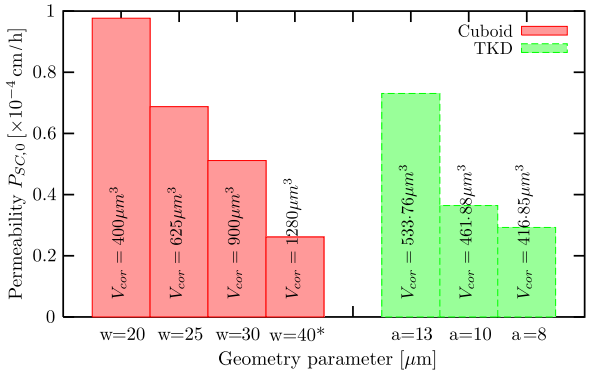

Fig. 7. The minimum permeability $P_{SC,0}$ for a reference value of $D_{lip} = 10^{-8}$cm^2/s on different geometries with $N = 10$ layers (cf. Table 2).

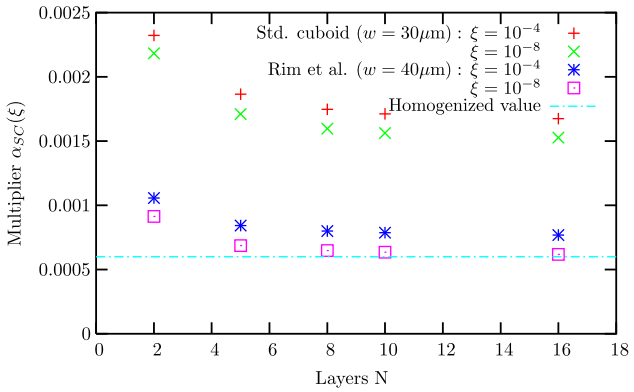

Fig. 8. Flux/permeability multiplier $\alpha_{SC}(\xi)$ depending on the number of layers N for the cuboid model geometries with $w = 30$ μm, $h = 1$ μm and $w = 40$ μm, $h = 0.8$ μm, respectively.

Though values for α_{SC} soon approach a limit, i.e., the value for a homogenized membrane, the multiplier for $N = 10$ layers still differs by about 5%, as can be seen when comparing to the values reported in [13] (straight line). The value of $\xi = 10^{-4}$ is chosen due to findings in the previous studies [26,27] for the model compounds flufenamic acid and caffeine, whereas $\xi = 10^{-8}$ represents a membrane with (almost) impermeable corneocytes.

5. Discussion

Since the mid seventies of the last century, it has been observed that the process of cell proliferation in the epidermis results in TKD-shaped cells in SC [1–4]. This is due to the fact that among all cells with constant volume, tetrakaidekahedral cells provide a surface configuration, which is close to the optimum [16,29]. Although this representation is still an approximation, it is morphologically more realistic than the cuboid model. This is further confirmed in the top view, cf. Fig. 3, which provides the hexagonal shapes typical of two-dimensional micrographs of epithelial cells [30,31].

Quantitative results are provided by high resolution imaging techniques [5,8]. However, compared to the in vivo or in vitro situation, some artifacts are likely to be included in the measurements, as pre-treatment and drying procedures were applied. Additionally, one has to account for intra-species variability. The parameterisation of the cells used in this work, which has an important impact on quantitative findings, should thus be interpreted as an educated guess, and the results should be discussed qualitatively first. The comparison of the three different model geometries in Fig. 5 shows that the ribbon geometry yields the best barrier with respect to permeability. However, this is the less realistic case: Due to the two-dimensional simplification, cells stretch infinitely into the direction, which is perpendicular to the plane of view in Fig. 1. Among the three-dimensional models, the TKD approach yields lower permeabilities at a comparable cell volume. The saw-tooth-like entanglement of the cells provides a better barrier than the brick-and-mortar-like structures. Note that horizontal overlap occurs on an intra-layer level for the TKD, whereas it is given on an inter-layer level for the ribbon and the cuboid model. As a consequence further, studies could also include more irregular polyhedra, e.g., trapezohedra. However, these approaches were disregarded in this study due to the lack of symmetry, which seems to contradict morphological differentiation.

In spite of the differences, the approximation for the permeability multiplier in Eq. (5) yields excellent agreements for all three geometry types. However, this is not derived within a rigid mathematical framework. Nevertheless, it also provides a tool to estimate the membrane's lag time, when used in combination with homogenization theory. Investigations on this subject are in progress.

6. Conclusion

This work performs a comparison of three different models for stratum corneum geometries (ribbon/cuboid/tetrakaidekahedra). Geometric parameters are estimated based on the literature data on human SC morphology. Permeabilities are then computed numerically. The study proves that the shape of the corneocyte cells has an important impact on the permeability of the membrane. Standard brick-and-mortar type models (ribbon, 2D) yield the lowest permeability values, but have an oversimplified and irrealistic geometry. The model based on tetrakaidekahedra (3D) shows permeabilities that are about twice larger, but the cell shape is closer to what is observed in reality. The three-dimensional cuboid model yields the largest permeabilities, compared to the TKD model they are about a factor two to three larger. In addition, the study at hand investigates the influence of the horizontal overlap, changes in the number of cell layers and of the corneocyte volume. It features permeability approximations (Eq. (5)), which are related to bio-physical quantities, such as partition- and diffusion-coefficients. Though the presented work is primarily of theoretical character, it provides insights that are relevant from a more practical point of view: Firstly, the results should prove useful in the field of dermal risk assessment of chemical exposure. Secondly, the study is supposed to contribute to the understanding of diseases resulting from skin disorders or from an altered cell morphology of the cells, like in psoriasis. As a last point, it should be stressed that the presented concept is not only aimed at different cell membranes, e.g., for plant parenchyma cells [32], but also can analogously be applied for all similar-type composite barrier membranes.

Acknowledgements

The authors thank Dirk Feuchter and Christine Wagner for providing the TKD-Modeller and the Cuboid-Modeller, respectively. Additionally, the authors thank Steffi Hansen, Saarland University, Saarbruecken for discussions regarding the morphology of the corneocytes. Parallel computations were performed on the SGI Altix 4700 system at the Leibniz-Rechenzentrum, Munich. Parts of this work were funded by the ZEBET division of the Federal Institute for Risk Assessment, Berlin.

References

[1] E. Christophers, H.H. Wolff, E.B. Laurence, The formation of epidermal cell columns, J. Invest. Dermatol. 62 (1974) 555–559.
[2] D.N. Menton, A liquid film model of tetrakaidekahedral packing to account for the establishment of epidermal cell columns, J. Invest. Dermatol. 66 (1976) 283–291.
[3] D.N. Menton, A minimum-surface mechanism to account for the organization of cells into columns in the mammalian epidermis, Am. J. Anat. 145 (1976) 1–22.
[4] T.D. Allen, C.S. Potten, Significance of cell shape in tissue architecture, Nature 264 (1976) 545–547.
[5] T. Richter, J.H. Müller, U.D. Schwarz, R. Wepf, R. Wiesendanger, Investigation of the swelling of human skin cells in liquid media by tapping mode scanning force microscopy, Appl. Phys. A 72 (2001) 125–128.
[6] T. Richter, C. Peuckert, M. Sattler, K. Koenig, I. Riemann, U. Hintze, K-P. Wittern, R. Wiesendanger, R. Wepf, Dead but highly dynamic – the stratum corneum is divided into three hydration zones, Skin Pharmacol. Physiol. 17 (2004) 246–257.
[7] J.A. Bouwstra, A. de Graaff, G.S. Gooris, J. Nijsse, J.W. Wiechers, A.C. van Aelst, Water distribution and related morphology in human stratum corneum at different hydration levels, J. Invest. Dermatol. 120 (2003) 750–758.
[8] N. Kashibuchi, Y. Hirai, K. O'Goshi, H. Tagami, Three-dimensional analyses of individual corneocytes with atomic force microscope: morphological changes related to age, location and to the pathologic skin conditions, Skin Res. Technol. 8 (2002) 203–211.

[9] M. Mihara, Scanning electron microscopy of skin surface and the internal structure of corneocyte in normal human skin. An application of the osmium-dimethyl sulfoxide-osmium method, Arch. Dermatol. Res. 280 (1988) 293–299.
[10] T.-F. Wang, G.B. Kasting, J.M. Nitsche, A multiphase microscopic diffusion model for stratum corneum permeability. I. Formulation, solution, and illustrative results for representative compounds, J. Pharm. Sci. 95 (2006) 620–648.
[11] D. Feuchter, M. Heisig, G. Wittum, Geometry model for the simulation of drug diffusion through the stratum corneum, Comput. Visual. Sci. 9 (2006) 117–130.
[12] C.E. Goodyer, A. Bunge, Numerical simulations compared against experimental results for barrier membranes with lithographically printed flakes, J. Membrane Sci. 306 (2007) 196–208.
[13] J.E. Rim, P.M. Pinsky, W.W. van Osdol, Using the method of homogenization to calculate the effective diffusivity of the stratum corneum with permeable corneocytes, J. Biomech. 41 (2008) 788–796.
[14] J.E. Rim, P.M. Pinsky, W.W. van Osdol, Using the method of homogenization to calculate the effective diffusivity of the stratum corneum, J. Membrane Sci. 293 (2007) 174–182.
[15] C. Wagner, Dreidimensionale digitale Rekonstruktion des humanen stratum corneum der Haut in Kombination mit Simulation substantieller Diffusion durch das stratum corneum, Ph.D. Thesis, Tierärztliche Hochschule Hannover, 2008 (in German).
[16] W. Thomson Lord Kelvin, On the division of space with minimum partitional area, Phil. Mag. 24 (1887) 503.
[17] D. Feuchter, M. Heisig, Y. Liu, G. Wittum. Simulation der Arzneimitteldiffusion durch das stratum corneum. I. Geometrie- und Gittererzeugung mit Tetrakaidekaedern, WiR Preprint, Heidelberg University, April 2004 (in German).
[18] D. Feuchter, Geometrie- und Gittererzeugung für anisotrope Schichtengebiete. Ph.D. Thesis, Heidelberg University, 2008 (in German).
[19] R.L. Anderson, J.M. Cassidy, Variation in physical dimensions and chemical composition of human stratum corneum, J. Invest. Dermatol. 61 (1973) 30–32.
[20] P.V. Raykar, M.C. Fung, B.D. Anderson, The role of protein and lipid domains in the uptake of solutes by human stratum corneum, Pharm. Res. 5 (1988) 140–150.
[21] M. Heisig, R. Lieckfeldt, G. Wittum, G. Mazurkevich, G. Lee, Non steady-state descriptions of drug permeation through stratum corneum. I. The biphasic brick-and-mortar model, Pharm. Res. 13 (1996) 421–426.
[22] M.E. Johnson, D. Blankschtein, R. Langer, Evaluation of solute permeation through the stratum corneum: lateral bilayer diffusion as the primary transport mechanism, J. Pharm. Sci. 86 (1997) 1162–1172.
[23] A.M. Barbero, H.F. Frasch, Transcellular route of diffusion through stratum corneum: results from finite element models, J. Pharm. Sci. 95 (2006) 2186–2194.
[24] P. Bastian, K. Birken, K. Johannsen, S. Lang, N. Neuss, H. Rentz-Reichert, C. Wieners, UG – a flexible software toolbox for solving partial differential equations, Comput. Visual. Sci. 1 (1997) 27–40.
[25] N. Neuß. Homogenisierung und Mehrgitter. Ph.D. Thesis, Heidelberg University, 1996 (in German).
[26] S. Hansen, A. Henning, A. Naegel, M. Heisig, G. Wittum, D. Neumann, K.H. Kostka, J. Zbytovska, C.M. Lehr, U.F. Schaefer, In-silico model of skin penetration based on experimentally determined input parameters. Part I: experimental determination of partition and diffusion coefficients, Eur. J. Pharm. Biopharm. 68 (2008) 352–367.
[27] A. Naegel, S. Hansen, D. Neumann, C.-M. Lehr, U.F. Schaefer, G. Wittum, M. Heisig, In-silico model of skin penetration based on experimentally determined input parameters. Part II: mathematical modelling of in-vitro diffusion experiments. Identification of critical input parameters, Eur. J. Pharm. Biopharm. 68 (2008) 368–379.
[28] E.L. Cussler, S.E. Hughes, W.J. Ward, R. Aris, Barrier membranes, J. Membrane Sci. 38 (1988) 161–174.
[29] D. Weaire, R. Phelan, Cellular structures in three dimensions, Philos. Trans. R. Soc. Lond. A 354 (1996) 1989–1997.
[30] M.C. Gibson, A.B. Patel, R. Nagpal, N. Perrimon, The emergence of geometric order in proliferating metazoan epithelia, Nature 442 (2006) 1038–1041.
[31] T. Lecuit, P.-F. Lenne, Cell surface mechanics and the control of cell shape, tissue patterns and morphogenesis, Nat. Rev. Mol. Cell Biol. 8 (2007) 633–644.
[32] J.D. Gray, P. Kolesik, P.B. Hoj, B.G. Coombe, Confocal measurement of the three-dimensional size and shape of plant parenchyma cells in a developing fruit tissue, Plant J. 19 (1999) 229–236.